Effect of graphitic inclusions on the optical gap of tetrahedral amorphous carbon films

K. B. K. Teo,[a] S. E. Rodil, J. T. H. Tsai, A. C. Ferrari, J. Robertson, and W. I. Milne
Engineering Department, University of Cambridge, Trumpington Street, Cambridge
CB2 1PZ United Kingdom

High sp^3 fraction tetrahedral amorphous carbon (ta-C) films can be prepared using the filtered cathodic vacuum arc (FCVA). A by-product of the deposition process are small micrometer sized graphitic particles which are also incorporated into the film. The particle coverage of FCVA films is typically $<5\%$, and thus the effect of these graphite inclusions have been largely ignored in earlier optical gap measurements of ta-C. By incorporating a better filter design (e.g., S-bend filter), the particle coverage can be reduced to 0.1%. In this article, we show that the effect of these graphitic inclusions is to scatter or absorb light which significantly affects the optical gap measurement and hence reduces the ''apparent'' optical gap of the ta-C film. By comparing two ta-C films with different particle coverage but the same sp^3 content of 85%, we show that we can correct for the effect of these inclusions. Our results confirm that the E_{04} gap of a 85% $sp^3 ta$-C matrix is 3.6 eV. The importance of considering these micro particles is emphasized as we find that for every 1% of area covered by particles, there is a 3–4 fold percentage difference between the corrected optical gap and measured gap of the film. © *2001 American Institute of Physics.*
[DOI: 10.1063/1.1351863]

I. INTRODUCTION

Diamond-like carbon (DLC) is defined as a form of amorphous carbon or hydrogenated amorphous carbon containing a high fraction of sp^3 bonds.[1] These DLC films are technologically interesting because they are relatively easily deposited at room temperature and possess some of the exceptional properties of diamond such as chemical inertness, mechanical hardness and semiconducting properties. Tetrahedral amorphous carbon (ta-C), a form of DLC with no hydrogen and up to 85% sp^3 bonding, is commonly deposited using a filtered cathodic vacuum arc (FCVA).[2] The deposition mechanism and characterization of these films have been reviewed elsewhere.[3,4] This article concentrates on the optical gap properties of ta-C films deposited by FCVA.

The electronic structure of amorphous carbon is determined by its sp^3 and sp^2 bonding. Robertson and O'Reilly[5] showed that amorphous carbon is a two-phase material where the σ bonds of sp^3 and sp^2 sites give rise to the σ valence and σ^* conduction band states. These σ and σ^* states are separated by a wide band gap (5.5 eV) as in diamond. The sp^2 sites in the ta-C matrix introduce π valence and π^* conduction states within the $\sigma-\sigma^*$ gap. These states form inner band edges and control the optical gap. The π states are stabilized by forming parallel oriented pairs and gain further energy by fusing into clusters of aromatic rings. These general results led to the cluster model of amorphous carbon, which proposed that sp^2 and sp^3 sites segregated into sp^2 clusters embedded in a sp^3 bonded matrix. The cluster model was initially proposed to explain the small gap

(1–2 eV) observed in a-C:H films, since big clusters of aromatics rings were believed to be the only units able to account for such small gap. Early measurements of $\sim 85\%$ sp^3 bonded ta-C material prepared by FCVA have determined the optical gap to be between 2–2.5 eV.[3,6] It is questionable, however, if the cluster model could be extended to explain the rather low measured optical gap of ta-C prepared by FCVA. The rate of energy gain by clustering is much lower than the disorder introduced by the deposition conditions used for these ta-C films.[7] Thus, the sp^2 sites are unlikely to form large clusters, as noted by molecular dynamics calculations.[8–10] The lack a D peak in the Raman spectra of as deposited ta-C films[11] also confirms experimentally that large clusters do not exist in ta-C. Lee *et al.*[12] showed that the band gap could be controlled by the distortion of small rings or chains, instead of the size of the clusters. It has also been shown empirically that the band gap of all forms of a-C and a-C:H depend on the sp^2 fraction. Generally, the band gap decreases as the sp^2 fraction increases:[7,11,13,14] We thus do not expect 85% sp^3 bonded ta-C prepared by FCVA to exhibit such a low optical gap of 2–2.5 eV.

In this article, we present another parameter which has a strong effect on the measured optical gap of ta-C films deposited by the FCVA technique. In a vacuum arc discharge, particles are ejected from the arc source together with ions and electrons[15] which form the plasma for deposition. The implementation of a 90° magnetic filter[16] can remove much of the macro-sized particles from the plasma. However, depending on the filter efficiency, it is still possible to find micron and submicron sized particles arriving at the substrate. To improve the filtering of these micron and submicron particles, double bend filters have been developed.[17] The carbon films deposited by FCVA are thus a composite of

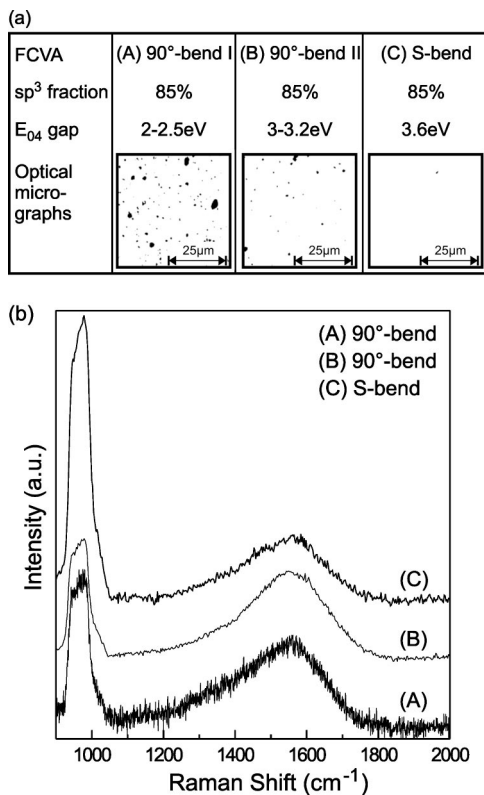[a]Author to whom correspondence should be addressed; electronic mail: kbkt2@eng.cam.ac.uk

FIG. 1. (a) *ta*-C films produced from FCVAs with different filters can have the same sp^3 content in the matrix but different measured optical E_{04} gaps. (b) Raman spectroscopy shows that there is little or no clustering (lack of D peak) in the *ta*-C matrix. It is clear that the microparticle inclusions affect the optical gap measurement since the *ta*-C matrix in all three cases is essentially the same.

micron sized graphitic particles dispersed in an amorphous *ta*-C matrix. In areas which do not have graphitic inclusions, the *ta*-C matrix is in fact extremely smooth. Recent measurements with a scanning tunneling-microscopy over a 400 nm×400 nm area have shown that the rms roughness is only 1.3 Å (peak to peak 8 Å).[18]

The effect of micrometer-sized graphitic inclusions on the measured optical gap is clearly illustrated in Fig. 1(a). Column A presents data obtained from a *ta*-C film deposited with a 90°-bend FCVA system. The optical gap ranges from 2 to 2.5 eV for films with 85% sp^3. Column B presents data from another 90°-bend FCVA but with a better filter design. The band gap obtained for 85% sp^3 is from 3–3.2 eV. Finally, column C corresponds to data obtained from a *ta*-C film produced by an S-bend filter. The sp^3 content in these film is again 85%, however, the band gap for the corresponding film is 3.6 eV. The three films shown in Fig. 1 have a different optical gap despite having the same sp^3 fraction. The visible micro-Raman spectra of the matrix of the three films, as shown in Fig. 1(b), can be fitted with a Breit–Wigner–Fano line without a D peak.[11] This verifies that there is no clustering in the matrix.[11]

It must be noted that in order to determine the sp^3 fraction, transmission electron energy loss spectroscopy (EELS) is performed using a submicron probe to avoid the microparticles. Therefore, the sp^3 content corresponds to the *ta*-C matrix. Similarly, Raman spectroscopy is performed by

micro-Raman in a clean area of the sample. However, when optical measurements are carried out, a much larger area is usually being examined and this area ranges from 0.1 to 1 mm in diameter depending on the beam size of the light source/laser in the measurement instrument. In this much larger area, the effects of light absorption or scattering from the graphitic inclusions become significant in determining the optical absorption properties of the *ta*-C matrix.

II. EXPERIMENTAL METHOD

ta-C films of ~30 nm were deposited on quartz substrates from two FCVA systems with different types of filters. One FCVA deposition system utilized a 90°-bend filter whereas the other system had an S-bend (off plane double bend type) filter. The *ta*-C films were prepared under conditions which yielded the same sp^3 content in both systems. Transmission EELS was performed using a 400 nm probe to confirm the sp^3 fraction of the *ta*-C matrix.

For optical absorption measurements, an UV-visible spectrometer with a light beam area of 2 mm^2 normally incident to the substrate was used. The transmittance ($T_{experiment}$) and reflectance ($R_{experiment}$) spectra of the *ta*-C film on the quartz substrate were measured. For the case of homogeneous materials with smooth surfaces in which scattering losses are negligible, traditional expressions for transmittance ($T_{calculated}$) and reflectance ($R_{calculated}$) for a thin film on a thick nonabsorbing substrate can be obtained by relating the refractive index (n) and extinction coefficient (k) with the Fresnel transmission and reflection coefficients. n and k are determined by solving iteratively the system of equations

$$T_{calculated}(n,k,\lambda) - T_{experiment}(\lambda) = 0, \qquad (1)$$

$$R_{calculated}(n,k,\lambda) - R_{experiment}(\lambda) = 0, \qquad (2)$$

where $T_{calculated}$ and $R_{calculated}$ are calculated values over the parameter space for n, k, and λ. Multiple solutions for n and k are a usual problem in this type of calculation. However, when $R_{experiment}$ and $T_{experiment}$ are measured under the same conditions, the multiple solutions for k do not deviate considerably from the true values, so that the problem is mainly restricted to the refractive index. For this, we determine the n of a sample deposited simultaneously on Si by a separate technique, namely fixed wavelength ellipsometry at 632.8 nm. This complementary data for n assists us in choosing the correct n solution.

The absorption coefficient, α, was then obtained using the dispersion relation

$$\alpha = \frac{4\pi k}{\lambda}, \qquad (3)$$

where λ is the wavelength in nanometers.

The optical gap of an amorphous semiconductor is conventionally defined as the energy (E_{04}) at which the absorption coefficient, $\alpha = 10^4$ cm^{-1}.

The films were also examined under a high resolution optical microscope (up to 1000×) fitted with a high-resolution charge coupled device camera (1280×1024 pix-
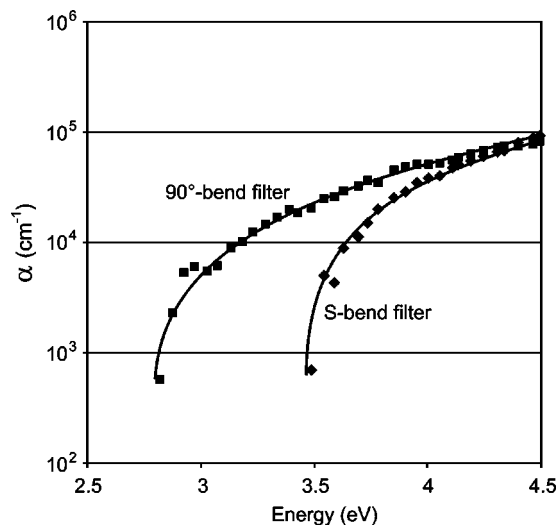
FIG. 2. The optical absorption coefficient (α) is plotted against photon energy for the 90°-bend filter film and the S-bend filter film.

FIG. 3. Optical micrographs of the 90°-bend filter film and the S-bend filter film are shown in (a) and (b), respectively.

els). Optical micrographs of the films were obtained and these were processed digitally to determine statistics for the in-film particles such as the area coverage and size distributions. The algorithm used scanned each pixel of the micrograph and compared the gray-scale value of the pixel with the background gray scale of the film. If the pixel was darker than the film, it was considered as a particle and its surrounding pixels were also examined to determine if it belonged to a group of pixels which constituted a larger particle. The entire micrograph was scanned pixel by pixel in this way to capture all the particles and their respective areas/sizes. The film prepared by the 90°-bend filter was also examined under a scanning electron microscope (SEM).

III. EXPERIMENTAL RESULTS AND DISCUSSION

The EELS measurements confirmed that the sp^3 content of the *ta*-C matrix of the films prepared from the 90°-bend filter and the S-bend filter were both 85%.[13] Assuming no scattering effects from the particles, the optical absorption coefficient versus photon energy plot is given in Fig. 2. The E_{04} gap of the films prepared by the 90°-bend filter and the S-bend filter are 3.15 and 3.6 eV, respectively. There is a clear reduction in the gap of the film prepared by the 90°-bend filter although the *ta*-C matrix of both films is essentially the same.

Figures 3(a) and 3(b) are optical micrographs of the films. Although both films appear to be smooth and transparent to the naked eye, black micrometer-sized particles are clearly visible when examined under the microscope. It is evident that the film prepared by the 90°-bend filter has a much higher microparticle density than the film prepared by the S bend. A larger area was examined for the S-bend filter film in order to deliberately capture more particles and obtain ''worst case'' particle statistics. The particle size distributions for both films are illustrated in Fig. 4(a) and the average size of the particles found on the films is 1 μm. The particle area coverage of the film produced by the 90°-bend filter and the S-bend filter are 3.22% and 0.01%, respec-
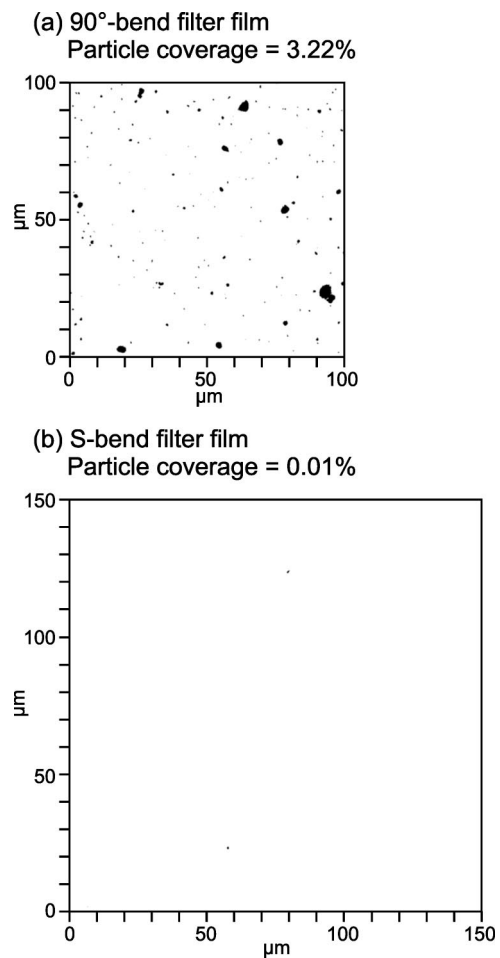
tively. The SEM image of the film produced by the 90°-bend filter [Fig. 4(b)] clearly shows the micrometer-sized particles at higher magnification.

We note that the microparticles appear dark in contrast to the *ta*-C matrix which is ''semitransparent.'' If light were transmitted by the microparticles, the microparticles would have appeared transparent. If light were reflected, the particles would have appeared shiny. Thus, to a first approximation, we can assume that no light has been transmitted or reflected wherever a black graphite particle is found on the film. The SEM image of the film shows that the particles are multifaceted flakes that are randomly oriented. Hence, incident light will be scattered in random directions due to the random orientation of faces of the particles when these particles are illuminated. The particles appear bright in the SEM as secondary electrons can easily escape from the edges/faces of the particles.

As a first approximation to the problem, the effect of light absorption or scattering from these particles can be accounted for by adjusting the $T_{\text{experiment}}$ and $R_{\text{experiment}}$ spectra accordingly. We assume that that the light incident on the randomly oriented microparticles is completely lost. This reduces the measured $T_{\text{experiment}}$ and $R_{\text{experiment}}$ spectra, and hence, both have to be scaled by an amount according to the

J. Appl. Phys., Vol. 89, No. 7, 1 April 2001
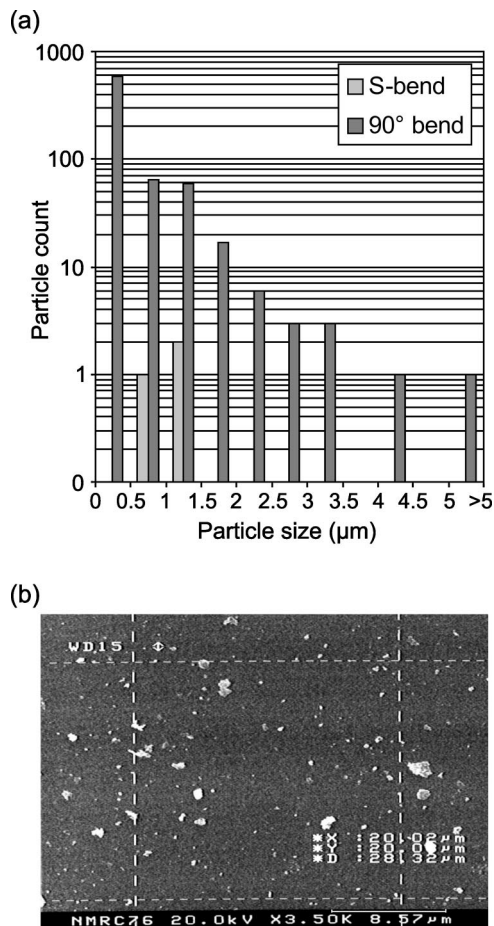
Teo *et al.* 3709

(a)

(b)

FIG. 4. (a) The particle size distribution histogram shown here is generated using the micrographs of Fig. 3. (b) The SEM image of the film prepared from the 90°-bend filter.

(a)

(b)

FIG. 5. (a) Corrected optical absorption coefficient (α) vs energy plots are derived for the 90°-bend filter film by taking into account various particle area coverages (1%–5%). (b) The E_{04} gap is plotted against the particle area coverage. For 3.22%, which is the particle area coverage of the 90°-bend filter film, the corrected gap of 3.57 eV corresponds well to the gap of the clean S-bend filter film of 3.6 eV.

percentage of the area (P) covered by the microparticles. We now define

$$T_{\text{corrected}} = T_{\text{experiment}}\left(\frac{1}{1-P}\right),$$

and

$$R_{\text{corrected}} = R_{\text{experiment}}\left(\frac{1}{1-P}\right). \tag{4}$$

These corrections (4,5) were applied to the original experimental transmittance and reflectance spectra of the 90°-bend film for values of area coverage from 1% to 5%. The absorption spectra were then rederived using the method detailed in Sec. II and the resultant spectra are plotted in Fig. 5. The corrected E_{04} gap increases with the particle area coverage as expected because the real gap should be higher than the measured gap if the particles are causing unwanted loss of the detected light signal. At a particle area coverage of 3.22%, the corrected gap is 3.57 eV which corresponds well to the 3.6 eV gap obtained with the ''clean'' film produced by the S-bend filter. The particle area coverage of 0.01% in the S-bend filter film does not affect the optical gap of the film significantly.

The error between the measured and corrected optical gap is plotted against the particle coverage in Fig. 6. For every 1% of area covered by particles, there is a 3–4 fold
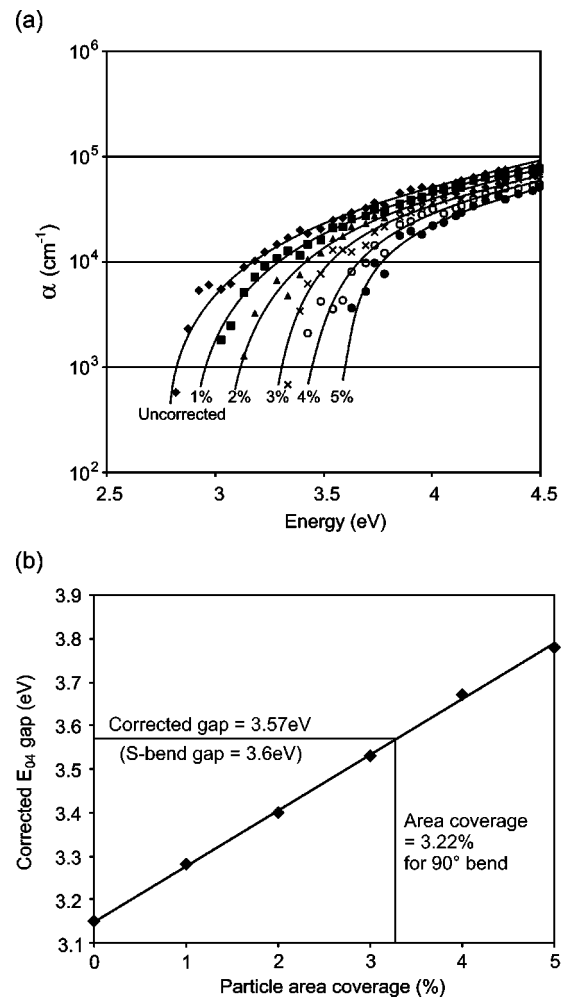
percentage difference between the corrected optical gap and measured optical gap of the film. This shows that the optical gap measurement is sensitive to small coverages of particles, which can only be reliably detected and characterized under a microscope.

Our correction method based on optical image analysis of the film is effective because the gap lies near the visible photon energy range. At other energies, the correction might not be effective because there will be an energy dependence absorption from the particles which will not correspond directly with the optical micrograph obtained in the visible energy range. It is also noted that the correction method might not be effective for high particle densities/area coverage because the particles, now spaced a few microns apart, form a randomly spaced diffraction grid which causes even more light loss.

IV. CONCLUSIONS

We have highlighted the importance of considering the scattering effects of micrometer-sized particles when
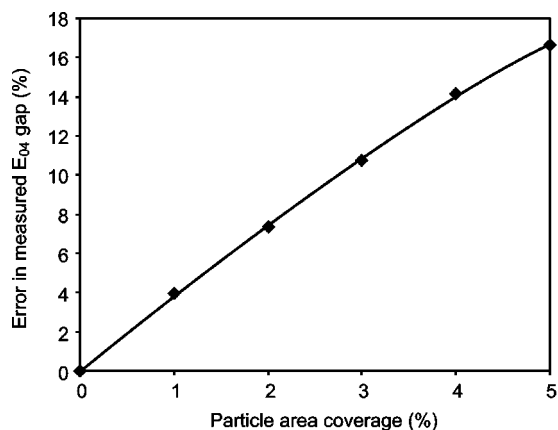
FIG. 6. The error in the measured optical gap is plotted against the particle area coverage. For every 1% of particle area coverage, there is a 3–4 fold error in the E_{04} gap measurement.

measuring the optical gap of *ta*-C films prepared by FCVA by photometric methods. Two *ta*-C films prepared from different filters can have the same sp^3 content but seemingly different optical gaps if the particle area coverage is not considered. The optical gap is shown to be similar for both films when the particle area coverage, computed directly from optical micrographs of the film, is used to correct the optical gap. This work can be extended to *ta*-C films prepared by pulsed laser deposition where micrometer-sized particles are also generated during deposition. The effect of these particles should also be considered in any optical measurement technique in which the probing area is large enough to ''capture'' the particles from the deposition process. We have also shown that the E_{04} gap of 85% sp^3 bonded *ta*-C is 3.6 eV.

[1] J. Robertson, Prog. Solid State Chem. **21**, 199 (1991).
[2] D. R. McKenzie, Rep. Prog. Phys. **59**, 1911 (1996).
[3] P. J. Fallon, V. S. Veerasamy, C. A. Davis, J. Robertson, G. A. J. Amaratunga, W. I. Milne, and J. Koskinen, Phys. Rev. B **48**, 4777 (1993).
[4] Y. Lifshitz, Diamond Relat. Mater. **8**, 1659 (1999).
[5] J. Robertson and E. P. O'Reilly, Phys. Rev. B **35**, 2946 (1987).
[6] M. Chhowalla, J. Robertson, C. W. Chen, S. R. P. Silva, C. A. Davis, G. A. J. Amaratunga, and W. I. Milne, J. Appl. Phys. **81**, 139 (1997).
[7] J. Robertson, Diamond Relat. Mater. **4**, 297 (1995).
[8] D. A. Drabold, P. A. Fedders, and P. Strumm, Phys. Rev. B **49**, 16415 (1994).
[9] T. Frauenheim, P. Blaudeck, U. Stephan, and G. Jungnickel, Phys. Rev. B **50**, 6709 (1994).
[10] N. A. Marks, D. R. McKenzie, B. A. Pailthorpe, M. Bernasconi, and M. Parrinello, Phys. Rev. B **54**, 9703 (1996).
[11] A. C. Ferrari and J. Robertson, Phys. Rev. B **61**, 14095 (2000).
[12] C. H. Lee, W. R. Lambrecht, B. Segall, P. C. Kelires, T. Frauenheim, and U. Stephan, Phys. Rev. B **49**, 11448 (1994).
[13] A. C. Ferrari *et al.*, Phys. Rev. B **62**, 11089 (2000).
[14] C. Oppedisano and A. Tagliaferro, Appl. Phys. Lett. **75**, 3650 (1999).
[15] J. M. Lafferty, *Vacuum Arc—Theory and Applications* (Wiley, New York, 1980).
[16] I. I. Aksenov, V. A. Belous, V. G. Padalka, and V. M. Koroshikh, Sov. J. Plasma Phys. **4**, 425 (1978).
[17] S. Xu, B. K. Tay, H. S. Tan, L. Zhong, Y. Q. Tu, S. R. P. Silva, and W. I. Milne, J. Appl. Phys. **79**, 7234 (1996).
[18] C. Arena, B. Kleinsorge, J. Robertson, W. I. Milne, and M. E. Welland, J. Appl. Phys. **85**, 1609 (1999).